

Investigation of Trends in T1 and T2 using Pulsed NMR at 15MHz

Abstract

The spin-lattice relaxation time (T1) and spin-spin relaxation time (T2) were measured in various samples to establish their trends with concentration in copper (II) sulphate solution (CuSO₄), with viscosity in glycerol, and with temperature in mineral oil. T1 measurements were made using an inversion recovery pulse sequence and T2 was measured using a Carr-Purcell-Meiboom-Purr (CPMG) Spin Echo pulse sequence with both sets of pulses being provided by a TeachSpin PS1/A pulsed NMR spectrometer. A relationship close to inverse proportionality was found between CuSO₄ and T1 and T2. The viscosity of glycerol was found to have a decreasing trend with both T1 and T2. Finally, it was found that each of T1 and T2 had a linear relationship with the temperature of mineral oil. These results agree with the currently accepted theory in the area. Additionally, the effects of using an off resonant frequency were studied. Here, the output signal amplitude varied as a sinc function with difference in frequencies as expected from the Fourier transform of the input pulse.

1 Introduction

The aim of the experiment was to investigate the phenomena of Nuclear Magnetic Resonance (NMR). Primarily this involved an investigation into the trends of T1, the spin lattice relaxation time, and T2, the spin-spin relaxation time, with the concentration of copper (II) sulphate solution (CuSO₄), the viscosity of glycerol and the temperature of mineral oil. Additionally, a secondary aim was to investigate the effects of using an off resonant input pulse. Both experiments were conducted using a TeachSpin PS1/A pulse NMR spectrometer.

In all of the primary experiments T1 was measured using an Inversion Recovery (IR) pulse sequence and T2 was measured using a CPMG spin echo sequence. Whilst other techniques exist to measure these parameters, for example, saturation recovery for T1[1], IR and Spin echo are both simple to implement within the PS1/A and provide a direct link to the use of T1 and T2 within Magnetic Resonance Imaging (MRI).

The values of T1 and T2 vary between different tissue types in the body[2] and MRI uses this variation to create contrast for certain tissues. Spin Echo and IR sequences are the basis of many techniques in MRI including

Diffusion Weighted Imaging and Short Tau Inversion Recovery respectively[3]. This demonstrates the importance of any investigation using these sequences.

The next section of the report will explain the relevant background theory. Section 3 will then discuss the methods used. The results are presented in section 4 and discussed in section 5. Conclusions are then summarized in section 6.

2 Background Theory

Protons are spin half particles and can behave like tiny bar magnets due to their magnetic moment. When placed in a uniform magnetic field, typically defined along the z direction, the protons will align either parallel or antiparallel to the field. There is an energy gap between the two states given by

$$\Delta U = \gamma \hbar B_0 = \hbar \omega_0 \quad (1)$$

where γ is the gyromagnetic ratio of the proton and B_0 is the strength of the magnetic field with the product of these defining the Larmor frequency, ω_0 . In a macroscopic system of many protons the energy levels are arranged with a Boltzmann distribution, resulting in a small excess aligned parallel to the field and a net resultant magnetization. This is illustrated in figure 1.

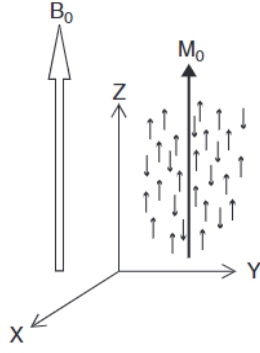


Figure 1: A uniform field, B_0 , is applied to a macroscopic sample of protons resulting in an overall magnetization M_0 aligned parallel to the field[3]

When a radio frequency (RF) pulse is applied perpendicular to the uniform field it perturbs the magnetization and causes it to precess around the z axis with a frequency of ω_0 due to gyroscopic motion[4]. To achieve resonance, the RF pulse must be corotating with the magnetization vector at ω_0 . This ensures that a constant torque is applied to the magnetization causing it to rotate towards the x - y plane. The amount of rotation is determined by the pulse width with a 90° pulse rotating the magnetization to the x - y plane and a 180° pulse, applied for double the time, rotating it to the $-z$ axis.

The application of a pulse changes the local magnetic field, and it takes time for the system to relax to thermal equilibrium again. This relaxation occurs via two mechanism[5].

The first is spin-lattice relaxation which has a decay constant of T_1 . This refers to the return of the magnetization vector from its rotation angle to the $+z$ axis. It is caused by the flipping of the spins between the two states which emits a photon of energy $\hbar\omega_0$. In general, T_1 is faster if the lattice has more states near the Larmor frequency. The decay is described by the Bloch equation

$$\frac{dM_z}{dt} = \frac{M_0 - M_z}{T_1} \quad (2)$$

where M_z refers to the component of magnetization along the z axis[6].

The second mechanism is spin-spin relaxation with a decay constant T_2 which refers to the dephasing of the spins in the x - y plane due to local inhomogeneities in the magnetic field. This is described by another Bloch equation

$$\frac{dM_{xy}}{dt} = \frac{M_0 - M_{xy}}{T_2} \quad (3)$$

where M_{xy} is the magnetization in the xy plane. Both mechanisms are illustrated in figure 2.

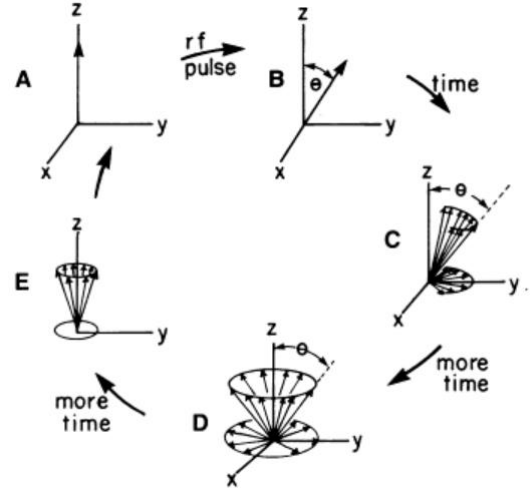


Figure 2: Illustration of the T_1 and T_2 decay processes. (A) The magnetization vector is in equilibrium along $+z$. (B) An RF pulse is applied to the system perturbing it to a flip angle of θ . (C) T_2 decay causes the perpendicular component to begin dephasing and they fan out in the x - y plane. (D) After more time the signal is fully dephased and the output signal is zero. (E) T_1 decay brings the flip angle back to zero and returns it to $+z$ where it reaches equilibrium again.[1]

However, due to engineering restrictions, the magnetic field is not perfectly uniform. The inhomogeneities in the field due to this lead to Free Induction Decay (FID) which has a decay constant of T_2^* . This is much quicker than T_2 and dominates the decay. The spin echo technique which is discussed in more detail in section 3.3 allows us to measure T_2 regardless.

For off resonant pulses, it is expected that the output signal amplitude will behave as a sinc function with the frequency difference between the RF pulse and Larmor frequency. This is due to the Fourier transform of the input pulse signal. More detail can be found in the appendix.

3 Methods

3.1 Initial Setup

All measurements were recorded on a picoscope with signals being generated by a TeachSpin PS1/A NMR spectrometer. This

was setup as recommended by the manual for the device[7].

Approximately 50 μ L of a sample was pipetted into an NMR tube that was placed in the magnet. This volume was kept consistent throughout to ensure the field experienced by the samples was consistent.

To check the system was at resonance the frequency of the input was adjusted until the mixing signal displayed no beats. The mixing signal measures the difference in frequencies between the Larmor frequency and the frequency of the RF pulse such that no beating indicates they are equal. It was found that the resonant frequency would drift during the day and regular checks and adjustments were made to ensure this caused no systematic errors.

The position of the sample in the magnet was adjusted until the FID peak amplitude and width were maximised. This ensured the sample was at the “sweet spot” of the magnet where the field was most uniform. O-rings were placed at the same height on the vials to ensure they were placed at the same height in the magnet. After sweet spot adjustment the resonant frequency was adjusted to account for the change in field.

The accuracy of the delay time was checked by comparing it to the delay time recorded on the oscilloscope between two 90° pulses. Across many different delay times it was found that the value measured on the oscilloscope was more precise than the resolution of the spectrometer. The errors on the delay time were therefore considered negligible compared to other considerations.

Throughout the experiment the repetition time was chosen to be at least 5T₁ of the sample such that at least 99% of the magnetization had fully decayed back to equilibrium[8] before a new pulse sequence. This would prevent systematic errors caused by the overlap of repeats.

3.2.1 T₁ Measurements for CuSO₄ and Glycerol

T₁ was measured using an IR sequence. The pulse sequence is a 180° pulse followed by a 90° pulse at a time τ later. The pulse angles were determined by eye such that the FID was maximised for 90° and zero for 180°. Solving equation 2 for these boundary conditions and recognizing that the magnetisation is proportional to the output signal, the output voltage, V, is given by

$$V = V_0(1 - 2e^{-\frac{\tau}{T_1}}) \quad (4)$$

where V₀ is the voltage after a 90° pulse. This can then be rearranged to the form of a straight line with a gradient of -1/T₁

$$\ln\left(1 - \frac{V}{V_0}\right) = -\frac{\tau}{T_1} + \ln(2) \quad (5)$$

The voltage was measured directly from the oscilloscope. There was a noticeable zero offset on the voltage signal and therefore a differential measurement between the offset and peak was used to negate this. Additionally, there was a significant amount of noise on the order of ± 0.1 V on the signal. Although this was reduced by removing the laptop charger it was an unavoidable random error due to the fluctuation of the peak height.

An example result is shown in figure 3 for 1.5625% CuSO₄ where T₁ was found to be 35.3 \pm 0.4ms with the overall error being given by the error in the gradient. The error bars get larger as the delay time increases. This is because 1-V/V₀ approaches zero so the log of this becomes unstable. Errors are lower when the log function is flatter at lower voltages. The missing data points occur where the peak height is too low in amplitude to distinguish from the noise.

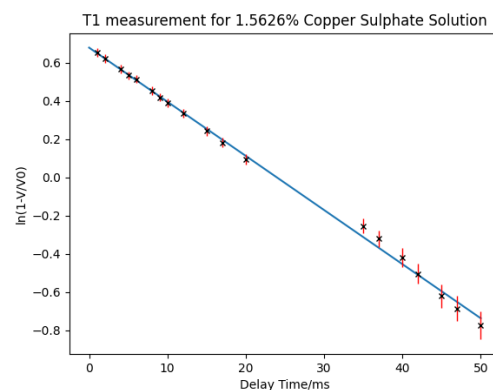


Figure 3: Plot for the measurement of T₁ in CuSO₄ with 1.5625% concentration using inversion recovery. T₁ was measured as 35.3 \pm 0.3ms.

Glycerol concentrations were converted to viscosities using formulas discussed by Cheng(2008)[9].

3.2.2 T1 of Mineral Oil Varying with Temperature

The method in 3.2.1 is inappropriate for measuring T1 in mineral oil. This is because it is slow to implement leading to large systematic errors due to cooling of the sample.

Instead, using equation 4 we can recognize that when $\tau = T1 \ln(2)$ the voltage will drop to zero. Therefore, T1 can be obtained with just one measurement, a far quicker technique ensuring the temperature is constant. The drawback is the large range in which the voltage appears undetectable as shown by figure 3. The delay time is therefore measured twice; when the voltage first disappears and when it reappears. The midpoint is used, and the range forms the error.

The temperature was changed using a water bath in a range of 20-60°C. The temperature was recorded before and after the T1 measurement with the mean being used as the value, and the range providing the error.

3.3 T2 Measurement of CuSO₄, Glycerol and Mineral oil

T2 was measured using a CPMG spin echo pulse sequence which is displayed in figure 4. After the initial 90° pulse the system decays with T2* due to FID. The dephasing effects of this are reversible and create an echo when they are rephased after the refocussing 180° pulse. The T2 effects due to spin interactions are irreversible and continue to decay creating

an overall envelope as shown in figure 4. Solving equation 3, the voltage of the envelope function is given by

$$V = V_0 e^{-\frac{t}{T_2}} \quad (6)$$

This can be rearranged to a straight-line format,

$$\ln(V) = \ln(V_0) - \frac{t}{T_2} \quad (7)$$

so that T2 can be determined by measuring the voltages of the echo peaks which lie on the T2 envelope.

The pulse angles were again determined by eye. The CPMG sequence is designed so any errors in the angle of the 180° pulse do not accumulate over the multiple applications of the pulse, avoiding systematic error. This is discussed more in the appendix.

Delay times were chosen so that there was no overlap between the peaks, this was judged by eye. Voltages were recorded from the oscilloscope as discussed in section 3.2.1, with errors on the peak heights arising due to the fluctuation from the noise.

Temperatures in mineral oil were changed using a water bath in the same range as 3.2.2. To ensure all the peaks were measured for the same temperature a screenshot was taken once the signal was displayed. This also minimised the measurement time and any cooling effects. The temperature was recorded before and after measurement with the midpoint being used and the range setting the errors.

Figure 5 shows an example result for glycerol with 12.5% concentration where T2 was

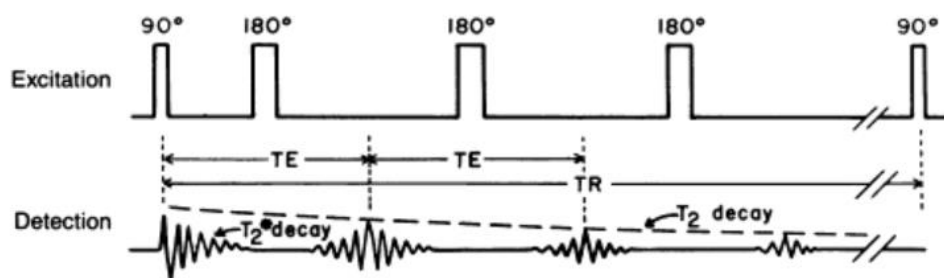


Figure 4: Spin-Echo pulse sequence and output signal. The top line shows the input RF pulse sequence, and the bottom line shows the output echo train. The dotted line represents the envelope on the echoes due to the irreversible T2 decay. TE is the time between echoes and TR is the repetition time[10].

measured as 179 ± 9 ms with the error coming from the error in the gradient. Unexpectedly, the data points do not appear as a straight line with the gradient becoming steeper with time. This was common to all samples of different concentration and contents.

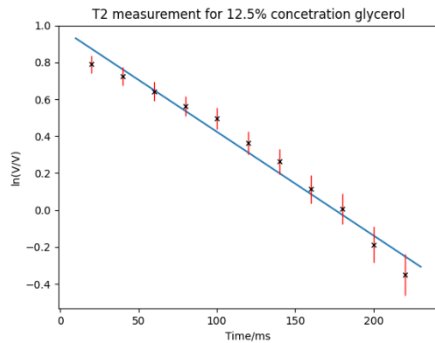


Figure 5: T2 measurement for 12.5% glycerol using a CPMG Spin-Echo. T2 was measured as 179 ± 9 ms.

No explanation was found for this despite additional checks the system was at resonance and the zero offset was accounted for. It was decided that it was caused by an unknown systematic error. As it appeared to affect all data consistently it was ignored when calculating a value of T2 from the gradient.

3.4 Measuring Off Resonance effects

Off resonance effects were measured by recording the voltage of a single 90° pulse. This was initially done at resonance and then the frequency was increased, and the process repeated. Data was collected as quickly as possible to minimise drift in resonance and voltages were recorded as described in section 3.2.1.

4 Results

4.1 Viscosity of Glycerol on T1 and T2

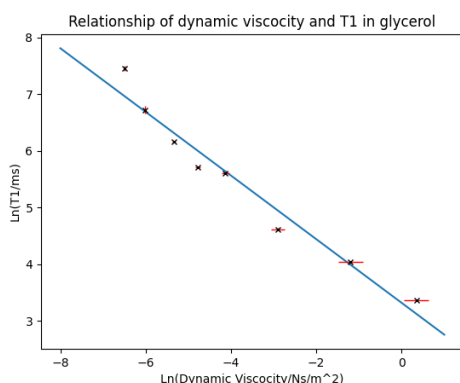


Figure 5: Plot of T1 against dynamic viscosity on a logarithmic scale. The gradient is -0.56 ± 0.05 .

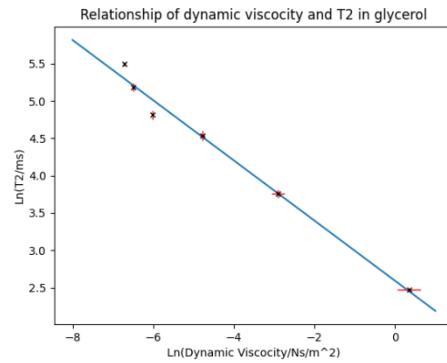


Figure 6: Plot of T2 against dynamic viscosity on a logarithmic scale. The gradient is -0.40 ± 0.03 .

Figures 5 and 6 show the relationship between T1 and T2 respectively with the dynamic viscosity of glycerol. The graphs are plotted on a log scale as this conveniently allows the data to be compared to an inverse proportionality relationship that is predicted by theory[11]. Although both data sets agree with a general trend that as the viscosity increases the decay time decreases; the gradients of the graphs are -0.56 ± 0.05 and -0.40 ± 0.03 which disagree significantly with the theoretical outcome of -1 for an inverse relationship.

The error in viscosity arises from the error in the concentration of the glycerol samples. These were not prepared as part of the experiment and therefore the error is unknown. All samples were estimated to have a 2% error. However, it is likely this was an underestimate given the number of outliers present in both figures.

4.2 CuSO₄ Concentration with T1 and T2

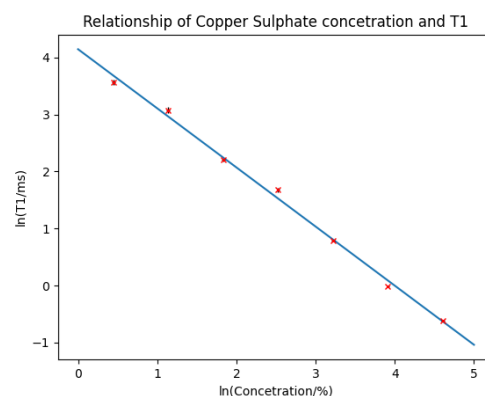


Figure 7: Plot of the relationship of T1 and the concentration of Copper Sulphate solution on a log scale. The gradient is -1.04 ± 0.03 .

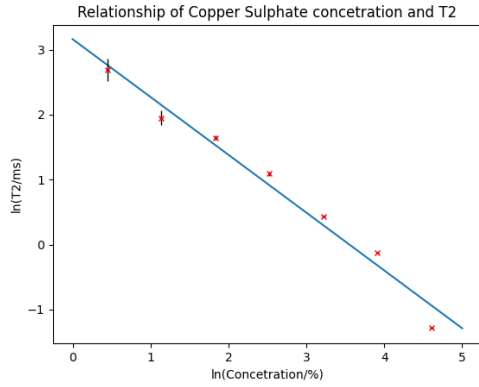


Figure 8: Plot of the relationship of T2 and the concentration of Copper Sulphate solution on a log scale. The gradient is -0.89 ± 0.06 .

Plots of the relationship between the concentration of CuSO_4 with T1 and T2 are shown in figures 7 and 8. These are again shown on a log scale to compare to the inverse proportionality relationship predicted by theory[11]. The gradients are -1.04 ± 0.03 and -0.89 ± 0.06 . Although the gradients do not match the -1 prediction within their error, the percentage difference is far less than the result for glycerol. The error in CuSO_4 concentration was assumed to be 2% in all samples.

4.3 Temperature of Mineral Oil with T1 and T2

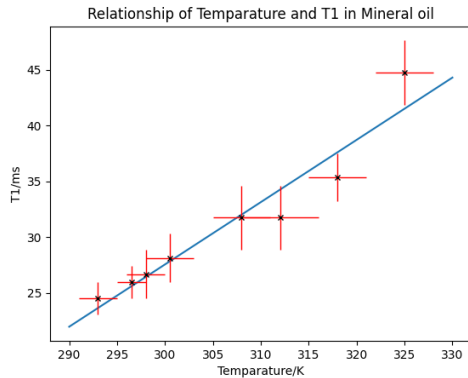


Figure 9: Plot of the relationship between T1 and temperature in mineral oil. It is found to be linear.

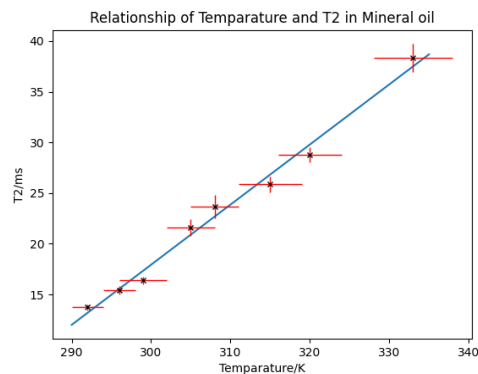


Figure 10: Plot of the relationship between T2 and temperature in mineral oil. It is found to be linear.

Figure 9 and 10 show plots of the relationship between temperature with T1 and T2 in mineral oil. These are both found to be linear relationships agreeing with the predicted theory[12].

4.4 Off Resonance Effects

As predicted, the relationship between voltage and the frequency difference to resonance is good fit to a sinc function which can be seen in Figure 11. An estimate for the pulse width can be determined from the first zero which occurs at $0.239 \pm 0.001 \text{ MHz}$. This is found to be $4.18 \pm 0.02 \mu\text{s}$.

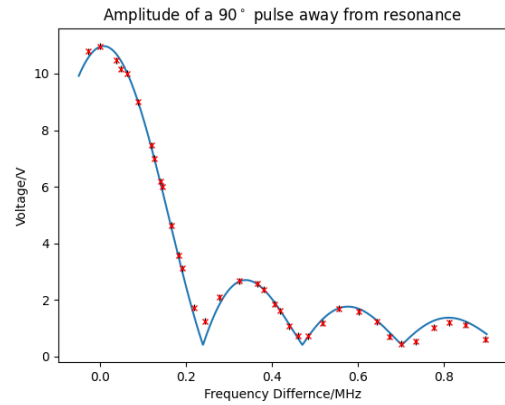


Figure 11: Plot of the off-resonance effects on the amplitude of a 90° pulse. A sinc function is fitted to the data and matches it well.

5 Discussion

In general, the trends in T1 and T2 are complex, depending on multiple factors simultaneously. In Bloembergen et al (1948)[11], it is shown that

$$\frac{1}{T_1} \propto \frac{N_{\text{ion}} T}{\eta} \quad (8)$$

Where N_{ion} is the number density of paramagnetic ions, T is the temperature and η is the viscosity. A similar relationship follows for T2 as we expect this to encompass both decay processes[4].

5.1 Glycerol Viscosity

Glycerol is diamagnetic and the experiment was completed at constant temperature suggesting the relationship should be dominated by viscosity. An inverse relationship is expected from equation 8

however the gradients are measured as -0.56 ± 0.05 and -0.40 ± 0.03 for T1 and T2 respectively differing significantly from the expected -1.

In reality, viscosity is not an isolated factor in this experiment. By changing the concentration of the sample, the local environment of the protons is also changed as well as their local molecular motions[11], independently of any viscosity effects. It is unlikely that an inverse relationship should be expected and the general trends that T1 and T2 decrease as viscosity increases are in fact sensible.

Additionally, there is uncertainty in the result due to the unverified concentrations of the glycerol samples. As suggested in section 4.1, it is likely that the errors on these concentrations were underestimated and may have produced a systematic error that was not accounted for.

5.2 CuSO₄ Concentration

The experiment was done at constant temperature, and the addition of copper ions to water does not change the viscosity significantly[12]. Paramagnetic ions, such as Cu⁺⁺, have unpaired electrons which create fields that interact with nearby nuclei. Due to the large gyromagnetic ratio of the electron compared to the nuclei they provide a powerful relaxation mechanism, explaining the expected inverse relationship[13]. This result was not found by the experiment to within the errors of the gradients, -1.04 ± 0.03 and -0.89 ± 0.06 for T1 and T2 respectively although the disagreement is not large at 4% and 11%.

Certain factors may explain these differences. For T2, it is likely there is a contribution from the unknown systematic error in the recording of results that was discussed in section 3.3. This made it difficult to accurately predict individual T2 values which may have affected the overall trend. Additionally, for both results the concentration of the samples were not verified creating another potential source of error.

5.3 Mineral Oil Temperature

This is a more complicated example as by increasing the temperature the molecules have extra energy to overcome attractive forces between them which decreases the viscosity. The expected outcome is more difficult to predict as there was no suitable method to directly measure the viscosity of the mineral oil at different temperatures. However, previous experimental work on vegetable oils[12], does suggest that the relationship should be linear agreeing with the experimental result.

6 Conclusions

A PS1/A NMR spectrometer was used to measure the trends in the spin-lattice relaxation time, T1, and the spin-spin relaxation time, T2, with the concentration of CuSO₄, the viscosity of glycerol and the temperature of mineral oil. The effects of using an off resonant frequency were also investigated.

It was found that T1 and T2 showed a relationship that was close to inversely proportional to the concentration of copper ions which had gradients of -1.04 ± 0.03 and -0.89 ± 0.06 when plotted on a log scale. The differences were assumed to be due to an unknown systematic error in the equipment found when measuring T2 values.

A general downwards trend was found between T1 and T2 and the viscosity of glycerol although an inverse relationship was expected. The difference was explained due to the changes in the local environment of protons in glycerol as the concentration was increased. Additional errors were incurred due to the unreliable concentrations of the glycerol samples. Any future experiments should verify the concentrations of all samples.

A linear relationship was found between T1 and T2 and the temperature of mineral oil. This agreed with previous experimental results, although future experiments may benefit by accounting for changes in the viscosity of the sample with temperature.

The effects of using an off resonant input signal were also verified and it was found that there was a sinc relationship between the output signal amplitude and the frequency difference between the RF pulse and Larmor frequency. This also agreed with theory.

References

- [1] Hendee W R, Morgan C J, (1984) “Magnetic Resonance Imaging Part I – Physical Principles”, West J Med. 141(4):491-500. PMID: 6506686; PMCID: PMC1021860.
- [2] Damadian R (1971) “Tumour detection by magnetic resonance” Science 171 1151-3
- [3] Sodickson A D, Sodickson D K, (2016), “Handbook of Neuro-Oncology Neuroimaging”, Chapter 18 “Introductory Magnetic Resonance Imaging Physics”, Academic Press
- [4] Ansorge R, Graves M, (2016) “The Physics and Maths of MRI”, Morgan and Claypool Publishers, ISBN978-1-6817-4068-3
- [5] Epstein S, Bohndiek S (2023), “Nuclear Magnetic Resonance- Part II experiment”, Laboratory Manual, Department of Physics, Cavendish Laboratory
- [6] Bloch F (1946) “The Nuclear Induction Experiment” Phys Rev 70 474-85
- [7] 1994, “Instructional Pulse NMR Apparatus”, Teachspin, instruction manual
- [8] Pykett I L, Rosen B R, Buonanno F S, Brady T J (1983), “Measurement of Spin-lattice relaxation times in nuclear magnetic resonance imaging”, Phys. Med. Biol. 28 723
- [9] Cheng N S(2008), “Formula for the viscosity of a glycerol-water mixture”, Industrial and engineering chemistry research, DOI: 10.1021/ie071349z
- [10] Hendee W R, Scherzinger A L, (1985), “Basic Principles of Magnetic Resonance Imaging – an Update”, West J Med. 143(6):782-92. PMID: 3911591; PMCID: PMC1306488.
- [11] Bloembergen N, Purcell E M, Pound R V (1948), “Relaxation effects in Nuclear Absorption”, Physical Review, Volume 73, Number 7
- [12] Nelson T R, Tung S M (1987), “Temperature dependence of proton relaxation times in vitro”, Magnetic Resonance Imaging, Volume 5, pages 189-199
- [13] Keeler J (2013) “Understanding NMR Spectroscopy”, University of Cambridge, Department of Chemistry

[14] Bloch F (1946) “Nuclear Induction” Phys Rev 70 460-74

Appendix

Output Signal From an Off Resonant Pulse

In NMR the output signal that is detected is from the weak RF signal emitted from precessing protons in the magnetic field, detected by external coils[14]. To understand the relationship the amplitude of this signal has with the frequency of the input RF pulse, it is easiest to consider the Fourier transform of the output and view the signal in the frequency domain. The Fourier transform is given by

$$f(\omega) = \int_{-\infty}^{\infty} f(t) \exp(-i\omega t) dt$$

where $f(\omega)$ is the output signal in the frequency domain, $f(t)$ is the output in the time domain and ω is the frequency of the RF pulse.

The output signal, $f(t)$, is the weak RF signal emitted by the protons which has a frequency of ω_0 . This can be written as

$$f(t) \propto \exp(-i\omega_0 t)$$

As the input RF pulse has a finite pulse width, a , the overall Fourier transform can be written as

$$f(\omega) \propto \int_{-\frac{a}{2}}^{\frac{a}{2}} \exp(i\Delta\omega t) dt$$

where $\Delta\omega = \omega_0 - \omega$. This has the solution

$$f(\omega) \propto \text{sinc}\left(\frac{\Delta\omega a}{2}\right)$$

The pulse width of the input RF pulse can then be estimated from the first zero of the sinc where $\Delta\omega = 2\pi/a$.

Elimination of Cumulative Errors Using the CPMG Spin Echo Pulse Sequence

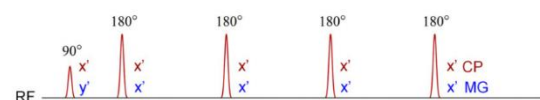


Figure 1: Comparison of the CP spin echo pulse sequence (shown in red) and the CPMG spin echo pulse sequence (shown in blue).[4]

Figure 1 shows a comparison between the CP spin echo pulse sequence and the CPMG spin echo pulse sequence. Both sequences use pulses of the same angles but the CPMG sequence introduces an additional 90° of phase between the initial 90° pulse and the first 180° pulse. This is indicated in the figure by applying the first pulse in the y direction rather than the x direction.

The issue with the CP sequence is that if the 180° pulse has an error in it, for example it is instead 175° , this error will accumulate each time the pulse is applied, becoming 10° then 15° etc in this example. This leads to large systematic errors over time as it is unlikely the RF pulse will be exactly 180° .

The additional phase introduced by the CPMG sequence counters this by ensuring that these errors are cancelled in each application preventing the error. Figure 2 shows the result of applying the CPMG sequence. If the refocussing pulse was 175° , the spins in figure 2d would be tilted around the x axis by 5° with the faster (blue) spins above the x-y plane and the slower (red) spins below it. This is exactly cancelled when the refocussing pulse is applied such that in figure 2h all the spins are in the x-y plane.

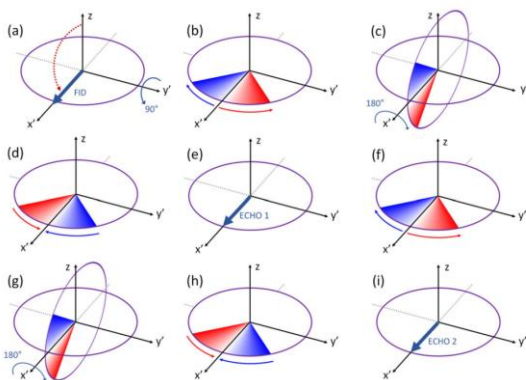


Figure 2: CPMG Spin-Echo pulse sequence. (a) A 90° pulse is applied causing the magnetization vector to flip 90° into the x-y plane. (b) FID occurs and the magnetization begins dephasing. (c) After a time τ a 180° pulse is applied reversing the directions of the vector in the x-y plane. (d) As the directions have reversed the dephasing of the magnetization now becomes rephasing. (e) At a time 2τ or TE the magnetization is fully rephased creating an echo in the signal. (f-i) The process is repeated with another 180° pulse leading to a second echo. [4]